

Environmental Earth Sciences

Investigating the Age Distribution of Fracture Discharge Using Multiple Environmental Tracers, Bedrichov Tunnel, Czech Republic.

--Manuscript Draft--

| | |
|--|--|
| Manuscript Number: | |
| Full Title: | Investigating the Age Distribution of Fracture Discharge Using Multiple Environmental Tracers, Bedrichov Tunnel, Czech Republic. |
| Article Type: | T.I. : DECOVALEX 2015 |
| Corresponding Author: | William Payton Gardner University of Montana Missoula, MT UNITED STATES |
| Corresponding Author Secondary Information: | |
| Corresponding Author's Institution: | University of Montana |
| Corresponding Author's Secondary Institution: | |
| First Author: | William Payton Gardner |
| First Author Secondary Information: | |
| Order of Authors: | William Payton Gardner Milan Hokr Hua Shao Ales Balvin Herbert Kunz Yifeng Wang |
| Order of Authors Secondary Information: | |
| Funding Information: | |
| Abstract: | The transit time distribution (TTD) of discharge collected from fractures in the Bedrichov Tunnel, Czech Republic, is investigated using lumped parameter models and multiple environmental tracers. We utilize time series of $\delta^{18}\text{O}$, $\delta^2\text{H}$ and $\delta^3\text{H}$ along with CFC measurements from individual fractures in the Bedrichov Tunnel of the Czech Republic to investigate the TTD, and the uncertainty in estimated mean travel time in several fracture networks of varying length and discharge. We compare several transit time distributions, including the dispersion distribution, the exponential distribution, and a developed TTD which includes the effects matrix diffusion. The effect of seasonal recharge is explored by comparing several seasonal weighting functions to derive the historical recharge concentration. We identify best fit mean ages for each TTD by minimizing the error-weighted, multi-tracer χ^2 residual for each seasonal weighting function. We use this methodology to test the ability of each TTD and seasonal input function to fit the observed tracer concentrations, and the effect of choosing different TTD and seasonal recharge functions on the mean age estimation. We find that the estimated mean transit time is a function of both the assumed transit time distribution and seasonal weighting function. Best fits as measured by the χ^2 value were achieved for the dispersive model using the seasonal input function developed here for two of the three modeled sites, while at the third site, the best fit was achieved with the exponential model and our seasonal input function. The average mean transit time for all TTDs and seasonal input functions converged to similar values at each location. The sensitivity of the estimated mean transit time to the seasonal weighting function was equal to that of the transit time distribution. These results indicated that understanding seasonality of recharge is at least as important as the uncertainty in the flow path distribution in fracture networks, and that unique identification of the TTD and mean |

| | |
|-----------------------------|--|
| | transit time is difficult given the uncertainty in the recharge function. However, the mean transit time appears to be relatively robust to the structural model uncertainty. The results presented here should be applicable to other studies using environmental tracers to constrain flow and transport properties in fractured rock systems. |
| Suggested Reviewers: | Painter Scott, PhD Oakridge National Laboratory painters@ornl.gov |
| | James McCallum, PhD james.mccallum@flinders.edu.au |

Opposed Reviewers:

Dear Editor,

The paper submitted here describes an investigation of the mean travel time in fracture networks estimated using multiple environmental isotope tracers. The focus is on determining the uncertainty in the derived mean travel time when different transit time distribution and different seasonal recharge weighting functions are used. The resulting analysis will be useful for future studies where environmental isotopes are used to estimate mean ages, and/or mean groundwater residence times are used to calibrate distributed flow and transport models. The data was provided as part of the DECOVALEX-2015 Task C2.

Thank you,

W. Payton Gardner

[Click here to view linked References](#)

Noname manuscript No.
(will be inserted by the editor)

1
2
3
4 **Investigating the Age Distribution of Fracture**
5 **Discharge Using Multiple Environmental Tracers,**
6 **Bedrichov Tunnel, Czech Republic.**
7
8

9
10 **W. Payton Gardner · Milan Hokr · Hua**
11 **Shao · Ales Balvin · Herbert Kunz ·**
12 **Yifeng Wang**
13
14

15 Received: date / Accepted: date
16
17
18
19
20
21
22
23
24

25 The work described in this paper was conducted within the context of the international DECO-
26 VALEX -2015 Project. The authors are grateful to the Funding Organizations who supported
27 the work. The views expressed in the paper are however, those of the authors and are not nec-
28 essarily those of the Funding Organizations. Technical University of Liberec (TUL) has been
29 supported by the Radioactive Waste Repository Authority of the Czech Republic (SURAO),
30 under contract no. SO2013-077. The results of the TUL authors were also obtained through
31 the financial support of the Ministry of Education of the Czech Republic (MSMT) from the
32 project LO1201 in the framework of the targeted support of the "National Programme for
33 Sustainability I". BGR's work was supported by the BMWi (Bundesministerium fr Wirtschaft
34 und Energie, Berlin). Sandia National Laboratory was supported under the DOE-Used Fuel
35 Disposition campaign. Sandia National Laboratories is a multi-program laboratory managed
36 and operated by Sandia Corporation, a wholly owned subsidiary of Lockheed Martin Corpo-
37 ration, for the U.S. Department of Energy's National Nuclear Security Administration under
38 contract DE-AC04-94AL85000.

39 W. Payton Gardner
40 University of Montana, Department of Geosciences,
41 32 Campus Dr #1296, Missoula MT, USA
42 Tel.: +1-406-243-2458
43 E-mail: payton.gardner@umontana.edu

44 Milan Hokr and Ales Balvin
45 Technical University of Liberec, Studentska 2, 46117 Liberec, Czech Republic

46 Hua Shao and Herbert Kunz
47 Federal Institute for Geosciences and Natural Resources, Stilleweg 2, 30655 Hanover, Germany

48 Yifeng Wang
49 Sandia National Laboratories, 1515 Eubank Blvd SE, Albuquerque NM, USA
50
51
52
53
54
55
56
57
58
59
60
61
62
63
64
65

Abstract The transit time distribution (TTD) of discharge collected from fractures in the Bedrichov Tunnel, Czech Republic, is investigated using lumped parameter models and multiple environmental tracers. We utilize time series of $\delta^{18}\text{O}$, $\delta^2\text{H}$ and ^3H along with CFC measurements from individual fractures in the Bedrichov Tunnel of the Czech Republic to investigate the TTD, and the uncertainty in estimated mean travel time in several fracture networks of varying length and discharge. We compare several transit time distributions, including the dispersion distribution, the exponential distribution, and a developed TTD which includes the effects of matrix diffusion. The effect of seasonal recharge is explored by comparing several seasonal weighting functions to derive the historical recharge concentration. We identify best fit mean ages for each TTD by minimizing the error-weighted, multi-tracer χ^2 residual for each seasonal weighting function. We use this methodology to test the ability of each TTD and seasonal input function to fit the observed tracer concentrations, and the effect of choosing different TTD and seasonal recharge functions on the mean age estimation. We find that the estimated mean transit time is a function of both the assumed transit time distribution and seasonal weighting function. Best fits as measured by the χ^2 value were achieved for the dispersive model using the seasonal input function developed here for two of the three modeled sites, while at the third site, equally good fits were achieved with the exponential model and the dispersion model and our seasonal input function. The average mean transit time for all TTDs and seasonal input functions converged to similar values at each location. The sensitivity of the estimated mean transit time to the seasonal weighting function was equal to that of the transit time distribution. These results indicated that understanding seasonality of recharge is at least as important as the uncertainty in the flow path distribution in fracture networks, and that unique identification of the TTD and mean transit time is difficult given the uncertainty in the recharge function. However, the mean transit time appears to be relatively robust to the structural model uncertainty. The results presented here should be applicable to other studies using environmental tracers to constrain flow and transport properties in fractured rock systems.

Keywords Environmental Isotopes · Hydrogeology · Isotope Geochemistry · Surface Water

1 Introduction

Flow and transport in fracture networks remains one of the more challenging issues facing hydrogeologists today. Accurate predictions of flow and transport in fracture networks is important in a variety of hydrogeological problems including: nuclear waste repository safety assessment, contaminant transport and remediation, unconventional hydrocarbon production, enhanced geothermal energy production and mine reclamation. Fractured reservoirs are characterized by extreme heterogeneity and data scarcity. Generally, it is not possible to uniquely determine the spatial distribution of fracture network properties and provide a complete description of the system behavior; however, simple models which incorporate field data at the appropriate scale, should be able to provide insight into the salient feature of the system behavior (Neuman, 2005). The transport time distribution is a

1 powerful description of the flow and transport in a hydrogeologic system; however,
2 little is known about the field scale transit time distribution in fracture networks.
3 Lumped parameter models provide a simplified methodology to investigate the
4 residence time distribution in fracture networks.
5

6 Transport in fracture networks is affected by rapid advection in fractures and
7 diffusion into and out of adjacent intact lower-permeability matrix (e.g. Haggerty
8 et al (2001); Maloszewski and Zuber (1990, 1985); Neretnieks (1980); Sudicky and
9 Frind (1982); Tang et al (1981)). The effect of matrix diffusion is to slow tracer
10 transport compared to the advective fluid velocity, dampen concentration variation
11 and produce long tailing of tracer release (Cook and Robinson, 2002; Maloszewski
12 and Zuber, 1985; Neretnieks, 1980, 1981). Tracer transport in fractured networks
13 has been evaluated theoretically and used to interpret tracer transport experiments
14 with a variety of models from analytical models of simple geometry to numerical
15 models of discrete fracture networks. Multiple continuum models allow linear ex-
16 change between the advective and immobile porosities for a single rate (Warren
17 and Root, 1963) to multiple mass transfer rates (Haggerty and Gorelick, 1995).
18 Analytical solutions exist for models that account for concentration gradients in
19 the matrix for simple geometries such as a single fracture (Tang et al, 1981), parallel
20 fractures (e.g. Maloszewski and Zuber (1990, 1985); Sudicky and Frind (1982))
21 and a distribution of different matrix block shapes and sizes (e.g. Haggerty et al
22 (2000)). Discrete fracture network models have been used to develop fully dis-
23 tributed reactive flow and transport models (e.g. Therrien and Sudicky (1996)) as
24 well as produce fluid velocity fields for particle tracking schemes which can be post
25 processed to account for matrix interactions (e.g. Painter and Cvetkovic (2005);
26 Painter et al (2008); Roubinet et al (2013)). The parameters used in these models
27 are a strong function of the spatial and temporal scale of interest (Neuman, 2005;
28 Shapiro, 2001), thus observations used to estimate fracture parameters should be
29 made at similar length and time scales to the desired predictions.

30 Environmental tracers can provide a rich dataset which can be used to un-
31 derstand fracture flow and transport over a wide range of spatial and temporal
32 scales. Environmental tracer concentrations have been used to develop conceptual
33 models of tracer transport, and constrain fracture network parameters in a vari-
34 ety of fractured rock systems. Cook and Robinson (2002) develop an analytical
35 model of environmental tracer transport in parallel fractures and show that tracer
36 concentrations could not uniquely determine fracture network properties, but were
37 capable of providing some constraint fracture spacing, aperture and recharge. Cook
38 et al (2005) use this model to constrain the recharge rate in a fractured, porous
39 aquifer in South Australia, and show that this simple model was a reasonable rep-
40 resentation of a more complex system and could be used prediction concentration
41 breakthrough.

42 Groundwater mean age can be used to characterize the residence time distribu-
43 tion in fracture networks. Analytical models of mean groundwater age have been
44 developed in fractured systems (Doyon and Molson, 2012). Groundwater age in
45 the field is often determined using environmental tracer concentrations. However,
46 in fracture networks, environmental tracer concentrations provide the solute resi-
47 dence time, which is not equal to the advective residence time (Neretnieks, 1981).
48 Thus, "apparent" groundwater ages determined from environmental tracers will be
49 older than the advective fluid residence time (Cook and Robinson, 2002), and the
50 use groundwater age in fractured systems must incorporate matrix interactions.
51
52
53
54
55
56
57
58
59
60
61
62
63
64
65

The residence time distribution is a fundamental characteristic of a flow system and provides critical information for determining the parameters controlling flow and transport in the system. Residence time distributions have been developed for a variety of simplistic aquifers (Cook and Herczeg, 2000; Maloszewski and Zuber, 1996). These models provide a convenient method to investigate the residence time and flow path distribution in hydrogeologic systems (e.g. Gardner et al (2010, 2011); Solomon et al (2010, 2015)). Lumped Parameter models in conjunction with tracer transport observations provide a means to investigate the residence time distribution and infer flow path characteristics in a reservoir (Danckwerts, 1953). Multiple environmental tracers can be used to identify the best age distribution and mixing models which best fit the observed data (Gardner et al, 2011; Solomon et al, 2010). McCallum et al (2014) show that age tracers have limited ability to uniquely identify the age distribution, but indicate the time series of tracers can help reduce uncertainty. Solomon et al (2010) indicate that the mean ages derived from multiple environmental tracers appears to be robust to choice the transit time distribution. However, these studies were carried out for porous flow aquifers and the application of lumped parameter models in fractured flow systems to estimate the transit time distribution is questionable.

The aim of this paper is to provide some insight into the uncertainty in estimating the mean transit time and the ability to distinguish the transit time distribution in fracture networks discharge to single fractures at the scale of 100's of meters using lumped parameter models and multiple environmental tracer concentrations. We utilize time series of $\delta^{18}\text{O}$, $\delta^2\text{H}$ and ^3H along with CFC measurements from individual fractures in the Bedrichov Tunnel of the Czech Republic to investigate the TTD in several fracture networks of varying length and discharge. We compare several transit time distributions, including a developed TTD which includes the effects matrix diffusion. We identify best fit mean ages for each TTD, and compare the ability of each TTD to fit the observed tracer concentrations and the effect of choosing different TTD on the mean age estimation.

2 Theory

Lumped parameter models were developed to investigate residence time distributions in chemical reactors where the true distribution of flow paths is not known (Danckwerts, 1953). The breakthrough curve of a tracer transported through the reactor can be used to provide information on the distribution of flow paths, and the processes affecting transport in the reactor, for example the amount of dead volume, the degree of mixing, and the amount of dispersion in 1-D flow in the reactor (Danckwerts, 1953). The residence time distribution has been used to investigate flow and transport in groundwater systems where the exact distribution of flow paths is unknown for many decades (e.g. Maloszewski and Zuber (1996)). The concentration at time t is given by the convolution integral:

$$C(t) = \int_0^\infty C_{in}(t - t')g(t')e^{-\lambda t'}dt', \quad (1)$$

where τ is the residence time, and λ is the decay constant of a radioactive tracer, $C(t - \tau)$ is the historical input at recharge and $g(\tau)$ is the residence time distribution for the flow paths discharging to the sampling point. Equation 1 along

1 with observations of tracer concentration in groundwater allows for the investigation
 2 of the distribution of flow paths and the processes affecting transport in the
 3 "black box" flow system which feeds the discharge point.
 4

5 **2.1 Residence Time Distribution**

6 The residence time distribution contains the flow and transport information for the
 7 system upstream of the sampling point and has been derived for several simplified
 8 aquifer types (Cook and Herczeg, 2000; Maloszewski and Zuber, 1996). Here we
 9 consider two existing transit time distributions which encompass two possible end
 10 members of reservoir types, and develop a distribution which incorporates matrix
 11 diffusion. The simplest age distribution considered is for water flowing along a
 12 single flow path or fracture subject to longitudinal dispersion, termed here as the
 13 dispersion distribution which can be written (Maloszewski and Zuber, 1982):
 14

$$15 \quad g(t') = t'^{-1} (4\pi P_e t' / \tau)^{-1/2} \exp \left[\frac{-\tau * (1 - t'/\tau)^2}{4P_e t'} \right], \quad (2)$$

16 where $P_e = D/vx$ is the system Peclet number with longitudinal dispersivity D ,
 17 velocity v and transport distance x , and τ is the mean transit time.
 18

19 An exponential distribution of residence times is achieved when there is complete
 20 mixing of an even distribution of flow paths of all ages, thus represents an
 21 end member where many different flow paths converge to the sampled fracture.
 22 The exponential distribution is written (Maloszewski and Zuber, 1982):
 23

$$24 \quad g(t') = \frac{1}{\tau} e^{-t'/\tau}. \quad (3)$$

25 Equations 2 and 3 were developed for porous media aquifers and do not consider
 26 the effect of diffusion into immobile regions on the transit time. In this study,
 27 a transit time distribution is developed that includes the effects infinite matrix
 28 diffusion for a constant fracture aperture. Here, we assume that the diffusion time
 29 to equilibrate matrix blocks with the fracture fluid is long compared to the changes
 30 in concentration, and that the fracture system is uniform.

31 The total transport time distribution ($g_{tran}(t_{tran})$) can be written as the convolution
 32 of the advective travel time distribution $g(t')$ and the retention time
 33 distribution ($g_{ret}(t_{ret})$) coupled by a velocity dependent transport resistant
 34 parameter distribution (Painter et al, 2008):
 35

$$36 \quad g_{tran}(t_{tran}) = \int_0^\infty \int_0^{t_{tran}} g_{ret}(t_{tran} - t' | \beta) f_{\beta|t'}(\beta | t') g(t') dt' d\beta, \quad (4)$$

37 where $t_{tran} - t' = t_{ret} \geq 0$ is the retention time from matrix diffusion and β
 38 is the spatially variable velocity dependent transport resistance parameter with
 39 a density distribution of $f_{\beta|t'}(\beta | t')$. If variability in the resistance parameter is
 40 neglected (Painter et al, 2008):
 41

$$42 \quad f_{\beta|t'}(\beta | t') = \delta(\beta - t' \bar{\beta} / \tau) \quad (5)$$

1 where δ is the Dirac function. In fractured rock applications, the resistance parameter is defined (Painter et al, 2008):
 2
 3

$$4 \quad 5 \quad 6 \quad \beta(t') = \int_0^{t'} \frac{ds}{b(s)}, \quad (6)$$

7 where b is the fracture half aperture and s is distance along the flowpath. If a
 8 constant aperture is assumed then (Painter et al, 2008):
 9

$$10 \quad 11 \quad 12 \quad \beta = \frac{t'}{\bar{b}} = t' \frac{\bar{\beta}}{\tau}, \quad (7)$$

13 where \bar{b} is the effective fracture aperture for the system of interest.
 14

15 Painter et al (2008) present retention time distributions for a wide variety
 16 of subsurface transport processes. For this paper, unlimited matrix diffusion is
 17 considered. The retention time distribution for infinite matrix diffusion is:
 18

$$19 \quad 20 \quad 21 \quad g_{ret}(t_{ret}|\beta) = \frac{\kappa\beta}{2\sqrt{\pi}t_{ret}^{3/2}} \exp\left[\frac{-\kappa^2\beta^2}{4t_{ret}}\right], \quad (8)$$

22 where $\kappa = \theta_{im}\sqrt{D_{im}}$, is a function of the matrix porosity θ_{im} and the matrix
 23 diffusion coefficient D_{im} .
 24

The concentration at time t for a system which includes matrix diffusion can
 25 now be written:
 26

$$27 \quad 28 \quad 29 \quad C(t) = \int_0^\infty C_{in}(t - t_{tran}) g_{tran}(t_{tran}) dt_{tran}. \quad (9)$$

30 Inserting equation 4 into equation 9 and assuming constant aperture and no vari-
 31 ance in the resistance transport parameter (equations 7 and 5) gives:
 32

$$33 \quad 34 \quad 35 \quad C(t) = \int_0^\infty C_{in}(t - t_{tran}) \int_0^{t_{tran}} g_{ret}(t_{tran} - t'|\beta)(t'/\bar{b})g(t')dt'dt_{tran}. \quad (10)$$

36 Equation 10 describes the transit time distribution, and the resulting concentration
 37 expected in fracture discharge at time t and is a function of the purely advective
 38 travel time, modified by retention from diffusion into the adjacent matrix. Here,
 39 flow along a single constant aperture fracture is considered, thus the advective
 40 travel time is assumed to the dispersive distribution (equation 2). Equation 10 is
 41 then parameterized by the mean advective travel time τ , the longitudinal disper-
 42 sivity P_e , the fracture aperture \bar{b} , matrix porosity θ_{im} and diffusivity D_{im} .
 43

2.2 Seasonal Input Function

44 The concentration input history $C_{in}(t)$ in equations 1 and 10 is the historical
 45 concentration of a given tracer in water recharging the aquifer system. The con-
 46 centration of these tracers is generally measured in precipitation and/or the at-
 47 mosphere. The concentration in recharge will be modified from the atmospheric
 48 or precipitation concentration by the processes occurring during recharge such as
 49 soil flow, evapotranspiration and seasonality of precipitation. When recharge is
 50

constant throughout the year, C_{in} will be equal to the concentration in precipitation. However, in cases where the concentration of the tracer changes seasonally – seasonality in precipitation, infiltration or evapotranspiration can cause C_{in} to differ from the atmospheric or precipitation record. These effects are especially important for stable isotopes of water and tritium. The annual flux weighted average concentration of tracer ($C_{in_{an}}$) is given by:

$$C_{in_{an}} = \frac{\sum_{i=1}^{12} C_i \alpha_i P_i}{\sum_{i=1}^{12} \alpha_i P_i}, \quad (11)$$

where $\alpha_i = R_i/P_i$ the recharge fraction is fraction of precipitation which become recharge for the i th month. In the area of the Bedrichov Tunnel winter is wetter and colder with precipitation predominantly falling as snow, and is a time of low evapotranspiration potential. During the summer months, precipitation falls as rain and there is a high evapotranspiration potential, thus there is a significant potential for seasonality in the recharge function.

To investigate the effects of seasonality we split the year into two seasons - summer and winter - and assume constant constant recharge fractions for summer months (α_s) and winter months (α_w). If the seasonal infiltration ratio $\alpha = \alpha_s/\alpha_w$ is defined, the seasonal recharge can be approximated by (Zuber and Maloszewski, 2001):

$$C_{in_{an}} = \frac{(\alpha \sum_{i=4}^9 C_i P_i)_s + (\sum_{i=10}^3 C_i P_i)_w}{(\alpha \sum_{i=4}^9 P_i)_s + (\sum_{i=10}^3 P_i)_w}, \quad (12)$$

where the summer months are assumed to be April through October and winter months November through March. The mean stable isotope composition of groundwater can be used to estimate α :

$$\alpha = \frac{(\sum_{i=3}^{10} P_i \delta_i)_w - \delta(\sum_{i=3}^{10} P_i)_w}{\delta(\sum_{i=4}^9 P_i)_s - (\sum_{i=4}^9 P_i \delta_i)_s}, \quad (13)$$

where δ is the mean groundwater isotope composition and sums are calculated for all winter and summer months on record.

The long term seasonal infiltration ratio α can now be used to estimate the seasonally weighted composition of recharge. This estimate has been done in variety of manners. The simplest and most common method is to use equation 12 to calculate the seasonally weighted annual average concentration. However, this limits the temporal resolution of the input function to annual steps. Interpretation of the high resolution sampling isotopic composition could provide information at sub-annual timescales, requiring a higher resolution input function. In this paper, seasonally weighted annual average precipitation along with three plausible monthly resolution input functions are investigated. The first and simplest high

resolution input function is simply the precipitation record, which inherently assumes $\alpha = 1$. The second infiltration function, taken from Zuber and Maloszewski (2001), is:

$$\delta_{in}(t) = \bar{\delta} + \alpha_i P_i (\delta_I - \bar{\delta}) / \sum_{i=1}^{12} \alpha_i P_i / n, \quad (14)$$

where $\bar{\delta}$ is the mean input (which must equal the mean output) and $\alpha_i = 1$ when $10 \geq i \leq 3$ and $\alpha_i = \alpha$ otherwise. We also develop another weighting function very close in form to equation 14:

$$\delta_{in}(t) = \bar{\delta} + \alpha_i P_i (\delta_I - \bar{\delta}) / \sum_{i=1}^{12} \alpha_i P_i. \quad (15)$$

The subtle difference between equations 14 and 15 is in the normalization term. Equation 14 is normalized by the average monthly recharge, thus recharge events greater than the average monthly recharge have much larger isotope shifts; however, this results in large fluctuations of the isotope composition when the precipitation is above the monthly average, and probably underestimates mixing in the vadose zone. Conversely, equation 15 is normalized by the total annual precipitation, which means that only months which comprise a significant amount of the total seasonally weighted total annual recharge can cause deviation from the seasonally weighted annual average recharge. This function produces a very smooth infiltration function very close to the seasonally weighted average concentration, but does allow large precipitation events to modify the input signal.

3 Study Area

The study location is a water supply tunnel which connects Josefuv dul reservoir with a water supply tunnel through the Jizera mountains in the northern Czech Republic. A description of the site can be found in *Hokr et al. this volume*. The tunnel is excavated through crystalline granitic rocks of the Krkonose-Jizera Composite Massif, a part of the Bohemian Massif of central Europe. The 2,600m tunnel was excavated in 1980-1981 with a maximum depth 200m below land surface (Figure 1). The tunnel has been utilized as a natural analogue underground laboratory for understanding fracture flow by the Czech radioactive waste disposal research group, RAWRA, since 2003.

Detailed geological history of the massif and characterization of the fracture network intersecting the tunnel are given in Zak et al (2009). The $\sim 1000 \text{ km}^2$ Krkonose-Jizera Plutonic Complex is dominated by the Jazira and Liberec course-grained porphyritic biotite granodiorite to granite. The tunnel lies in the Jaziera granite which is crosscut by two sets of steeply dipping roughly orthogonal fracture sets trending NE-SW and NW-SE. Fractures are roughly planar and subparallel and show little interaction with each other. Fracture spacing ranges from 1 cm to several meters with the most common spacing between 10 cm - 120 cm. Most fractures do not transmit measurable water discharge.

Fracture discharge and isotopic composition data were collected by the Technical University of Liberec and Czech Technical University in Prague respectively from 2010 to 2014 as part of the RAWRA characterization project. These data

were made available as part of the DECOVALEX 2015 project as part of a task to model flow and transport in fractured crystalline systems. Historical isotope composition of precipitation is available by leveraging the Uhliriska experimental watershed isotopes in precipitation database.

4 Field and Analytical Methods

Measurement of fracture discharge, water quality and temperature were at the sampling locations depicted in Figure 1. The irregularly spaced sampling intervals were chosen to be representative of different flow regimes in the tunnel (*Hokr et al. this volume*) (Figure 1). Manual measurements of fracture discharge were made at each site at 14 day intervals starting in 2006. Fracture discharge was measured using V-notch weirs or drip counting depending on the fracture discharge. Automatic measurements of fracture discharge at hourly intervals began in 2009. The locations of automatic measurement have continuously expanded since 2009, thus the density of data and sampling intervals vary for each sampling site. Automated measurements are verified by manual measurements at the 14 day intervals.

Stable isotope composition of fracture discharge at the sampling sites has been measured since 2010. Stable isotope samples were collected at 14 day intervals in 50 ml bottles and analyzed at the IAEA stable isotope laboratory in Vienna, Austria. Dissolved CFC's, tritium and dissolved noble gases were measured at the IAEA Isotope Hydrology Laboratory as part of an IAEA Technical Cooperation Project. Dissolved CFCs were collected in 250 ml glass bottles with metal caps completely submerged in buckets filled with fracture discharge. Dissolved CFC concentrations were measured using purge and trap gas chromatography. Tritium was collected in 1L bottles and analyzed by electrolytic enrichment and counting. Dissolved noble gases were collected using copper tube samples (Weiss, 1968) and analyzed using mass spectrometry.

5 Modelling Methods

The input concentration history $C_{in}(t)$ was estimated at the site for each tracer modeled. Stable isotopes in precipitation near the study site are available from the Uhliriska experimental watershed at monthly intervals beginning in 2006. In order to extend the precipitation data set back in time, the Vienna stable isotope in precipitation data set, the closest and longest time series in the IAEA Global Network of Isotopes in Precipitation was used to provide an estimate of the values in precipitation at the site from 1960 to 2006.

The seasonal recharge coefficient α was calculated for each modeled location using the average δD and $\delta^{18}O$ composition of the groundwater and average of Uhliriska dataset and using equation 13 to calculate an α for each isotope. The α used to create the seasonally weighted recharge concentration was taken the average of that calculated with each isotope. Seasonally weighted concentrations were then calculated for tritium, δD and $\delta^{18}O$ using raw historical precipitation and equations 12, 14 and 15 for each sampling site at monthly intervals. The input history for CFCs was calculated using the historical CFC mixing ratios in the atmosphere (Bullister, 2011), the average noble gas recharge temperature

1 estimate of 4.8 °C from IAEA tritium-helium analyses, a characteristic recharge
 2 elevation of 750 m, and zero excess air, to give the CFC concentration at each
 3 site in biannual intervals. In order to provide high enough temporal resolution
 4 to reduce numerical error the time were resampled at daily intervals using linear
 5 interpolation to give the discrete concentration input history \bar{C}_{in} .
 6

7 Equations 1- 10 were simulated using discrete convolution of linearly interpo-
 8 lated concentration input history (\bar{C}_{in}) and weighting function vectors (\bar{g}). Nu-
 9 merically efficient discrete convolution was accomplished using multiplication of
 10 the Fourier transformed discrete vectors. Convolution operations were written in
 11 python.
 12

13 Three of the sampling locations depicted in Figure 1 representative of: shallow
 14 high discharge (V6), deep low-discharge fracture discharge (V3), and deep large
 15 discharge (V4) were modeled. The concentration in discharge was modeled at each
 16 location using equations 1 with the dispersion and exponential weighting functions
 17 and 10 with the dispersion advective travel time distribution. At each modeled
 18 location, three different concentration input histories were evaluated (equations
 19 12, 14 and 15) using the methods described above.
 20

21 For each combination of weighting function and historical concentration his-
 22 tory, the best fit mean groundwater age at a sampling site was estimated by fitting
 23 the observed multi-tracer data at the site. Best fit estimation was accomplished
 24 by minimizing error weighted chi-squared residual using a Levenberg-Marquardt
 25 algorithm. The error mean age estimate was calculated from the 95% confidence
 26 interval of the covariance matrix, using the Jacobian of the error weighted chi-
 27 squared residual.
 28

6 Results

30 The best fit modeled age, uncertainty estimate and χ^2 fit are reported for each
 31 precipitation weighting function for each age distribution at all modeled fracture
 32 locations in Tables 1-2. At each location, the mean age and standard deviation
 33 in estimated age for each age distribution due to the different conceptualization
 34 of seasonal recharge function is summarized in Table 4. The mean age and the
 35 standard deviation in mean age estimates due to the assumed age distribution is
 36 reported for each input function in Table 5. The effect of increasing mean travel
 37 time on $\delta^{18}\text{O}$ signal, along with the observed values at the V6 sampling site,
 38 is shown for a dispersion TTD (equation 2), using the annual average weighted
 39 precipitation function (equation 11) is shown in Figure 2. As the age increases
 40 the variation in the $\delta^{18}\text{O}$ signal decreases. The corresponding effect on the CFC-
 41 12 concentration, along with observed data for the V6 sampling site is shown in
 42 Figure 3. During the multi-tracer inversion, the difference between all the observed
 43 tracer and the modeled signal is minimized by varying the mean transit time.
 44

45 Table 1 gives the summarized results for the V6 sampling site. The overall mean
 46 age for all age distributions and all recharge weighting functions is 4.58 years with
 47 a σ of 1.02 years. For the dispersive age distribution, the mean estimated age over
 48 all input functions is 3.4 years with a standard deviation (σ) of 2.6 years. The
 49 exponential age distribution gives a mean age of 5.0 years with a σ of 1.28 years
 50 for all input functions. For the matrix diffusion model, the mean total transit time
 51 is 5.33 years with a σ of 0.99 years for all input functions. In the matrix diffusion
 52
 53
 54
 55
 56
 57
 58
 59
 60
 61
 62
 63
 64
 65

1 model, the mean advective travel time is 2.55 year, with an average matrix diffusion
2 retention time of 2.78 years. The best fit to the observed data as measured by the
3 χ^2 residual was achieved by a dispersive age distribution with the seasonal input
4 function developed here (equation 15). The observed data and the overall best fit
5 modeled concentration for all tracers is shown in 4. Overall, the dispersion model
6 gives the best fits to the measured data; however, the variance in χ^2 over all the
7 precipitation input functions is high enough to encompass the χ^2 of the matrix
8 diffusion age distribution, indicating that it is difficult to tell the difference between
9 the two age distributions given the uncertainty in the input function (Table 4).

10
11
12 Table 2 summarizes the results for the V2 sampling site. The average mean
13 travel time (τ) over all age distributions and input functions is 7.86 years with a
14 σ of 2.2 years. For the dispersion age distribution, the average mean travel time is
15 10.3 with σ of 8.49. The exponential age function give an average mean travel time
16 of 6.06 with a σ of 2.1 years. For the matrix diffusion distribution, the mean total
17 transit time is 7.23 years with a σ of 2.3 years, with an average mean advective
18 travel time of 3.3 years and an average mean retention time of 3.9 years. The best
19 fit combination of models is the dispersion age distribution and input function 15.
20 The observed data and overall best fit modeled concentration for all tracers at
21 V2 is shown in Figure 5. Overall best fits are for the dispersion model followed
22 by the exponential and finally matrix diffusion models. The variance in χ^2 due
23 to uncertainty in the seasonal weighting function encompasses the fits of all other
24 travel time distributions, thus it is difficult to uniquely pick any of the travel
25 time distributions as the best (Table 4). For the seasonal weighting functions, the
26 overall best fit is given by the developed seasonal weighting function (equation
27 15). This weighting function clearly provides the best fits regardless of the travel
28 time distribution used (Table 5).

29
30
31 For the V4 sampling site, the overall average mean travel time is 6.56 years
32 with σ of 1.2 years for all travel time distributions and input functions (Table 3).
33 Average travel time for the dispersion distribution is 5.30 years with a σ of 2.13
34 years. Average travel time for the exponential age distribution is 6.7 years (σ 3.2
35 yr), and average travel time for matrix diffusion distribution is 7.74 (σ 3.2 yr). For
36 the matrix diffusion distribution the average advective mean travel time is 3.47
37 years and the average retention time was 4.3 years. The best fit combination was
38 our seasonal infiltration function (eq 15) with the dispersion equation; however,
39 this combination produces an anomalously low mean travel time of 3.55 years. The
40 observed data and overall best fit modeled concentration for all tracers at V4 is
41 shown in Figure 6. The exponential age distribution fits the data nearly as well
42 with an anomalously high mean travel time of 10.8 years. Over all the seasonal
43 weighting functions, the best fits were given by the exponential model, followed by
44 the dispersion model and finally the matrix diffusion model. At V4, uncertainty
45 in the input function creates enough variance in the χ^2 residual that the average
46 χ^2 values for each TTD are within error (Table 4), thus choosing the best age
47 distribution is difficult given the available data. As in the other models, the input
48 function developed in this paper provides better fits than the other input functions
49 regardless of the travel time distribution (Table 5).

50
51
52
53
54
55
56
57
58
59
60
61
62
63
64
65

1
2
3
4
5
6
7
8
9
10
11
12
13
14
15
16
17
18
19
20
21
22
23
24
25
26
27
28
29
30
31
32
33
34
35
36
37
38
39
40
41
42
43
44
45
46
47
48
49
50
51
52
53
54
55
56
57
58
59
60
61
62
63
64
65
7 **Discussion**

The results presented here highlight the difficulty in using tracer concentrations to constrain travel time in a fractured network system. At all sampling locations it is difficult to distinguish the best travel time distribution when considering different conceptualizations of the seasonally weighted input function. The inability to distinguish a single best age distribution using measured tracer concentration is consistent with the findings of McCallum et al (2014) and Solomon et al (2010). Thus, the estimated mean age is dependent upon the conceptualization of the system. The standard error of the mean travel time estimate (defined as the standard deviation of mean travel times normalized by the average mean travel time) over all travel time distributions and seasonal weighting input functions ranges from 19% at the V4 sampling site to 22.4% at the V6 sampling site. These results indicate that tracer derived mean travel times converge to a similar value consistent with Solomon et al (2010), and can still be used to provide significant constraint on the flow system.

A significant finding of this study is that the estimated mean travel time is as sensitive to the assumed seasonal input function as the travel time distribution. The effect of seasonality of recharge on the age estimate is largely unconsidered in most studies, and these results show that it is at least as important as the age distribution assumption. Seasonality of recharge may not have as large an effect on travel time estimates which use dissolved gas tracers when the recharge zone is deep enough to keep the recharge temperature constant. However, in situations where the water table is shallow and seasonality is pronounced, recharge temperatures can differ from the mean annual temperature (Thoma et al, 2011) and seasonality will affect dissolved gas tracers. For isotopes of water including tritium and thus tritium-helium age dating, seasonality of recharge will always be important. Mixing of recharging waters during infiltration is a classic and active question in hydrology (e.g. Evaristo et al (2015); Kennedy et al (1986)), and more investigation is need on the effect of seasonality on groundwater age determination. Of the seasonal recharge functions considered in this study, the developed formula consistently fits the observed data better than other functions. This function keeps the recharge concentration close to the annual average concentration, but allows large isotopic deviations in precipitation to effect the recharge concentration. While considerably more investigation is needed to validate this recharge function, the good fits here indicate that at least in this setting it appears give a reasonable approximation to the processes involved.

For two of the three model locations V6 and V2, the observed concentration were best fit by the dispersion travel time distribution. These sampling locations correspond to the discharge from individual fractures intersecting the tunnel at different depths. The shallowest sampling location V6 had the shortest travel time and the deeper sampling location, V2, had a longer travel time. The lumped parameter modeling is conceptually consistent with discharge from these fractures occurring a single fracture network, described a single flow path, rather a collection of multiple flow paths which mix together. For one of the locations, V4, the exponential age distribution fits the data as well as the dispersion model. At this location discharge from a larger fault system was sampled, thus a mixture of different flow paths with a range of ages (which the exponential model represents) is a likely conceptual model. However, uncertainty in the seasonal weighting function

1 makes it difficult to identify which of these transit time distribution best fits the
2 data.

3 The fact that the matrix diffusion model does not significantly improve fits
4 indicates that, given the travel times in this fracture network and representative
5 parameters controlling matrix diffusion, matrix diffusion is not a dominant process
6 controlling transport in these fractures. The lack of significant matrix diffusion is
7 also highlighted by the relatively small difference between the mean transport
8 time including matrix diffusion and the mean advective only travel time (Tables
9 1-2). While the effect of matrix diffusion appears small on the mean travel time
10 in this study, we expect that matrix diffusion would play a much stronger role in
11 controlling the initial arrival and tailing properties of the transit time distribution,
12 which are likely not identifiable using tracer concentrations (McCallum et al, 2014).
13 Additionally, in environments with stronger matrix diffusion (e.g. high matrix
14 porosity and/or longer travel times), the matrix diffusion transit time distribution
15 developed here will be useful in modeling the total transit time.

17 8 Conclusion

18 In this study, we investigate the transit time distribution in fracture networks dis-
19 charging to individual fractures of the Bedrichov Tunnel in the Czech Republic
20 using time series of stable isotopes of water and tritium along with synoptic dis-
21 solved CFC concentrations. We use lumped parameter models to compare some
22 likely transit time distributions and determine the effect of transit time distribu-
23 tion and seasonal input choice on the estimated mean age. We compare residence
24 time distribution for a single advective path with longitudinal dispersion, complete
25 mixing (exponential age distribution) and a newly developed a residence time dis-
26 tribution for 1D advective-dispersive transport with infinite matrix diffusion. In
27 order to investigate the effect of seasonal recharge, we compare uniform infiltration,
28 a weighting function developed in Zuber and Maloszewski (2001), and a weighting
29 function developed in this paper. We find that the modeled concentrations are de-
30 pending upon the transit time distribution and the seasonal infiltration weighting
31 function, and that the estimated mean travel time is as sensitive to the choice
32 of seasonal weighting function as that of the transit time distribution. Given the
33 uncertainty in the seasonal weighting function, it is difficult to completely identify
34 the best fit transit time distribution. However, regardless of the age distribution
35 or the infiltration model chosen, the best fit mean age converges to a similar value
36 for all three locations modeled here. These results indicate that lumped parame-
37 ter models along with multiple environmental tracers can be used constrain the
38 mean age, and develop some information on the transit time distribution to help
39 develop conceptual models of flow and transport in fracture networks. The re-
40 sults and methods presented should be applicable in other fractured crystalline
41 environments.

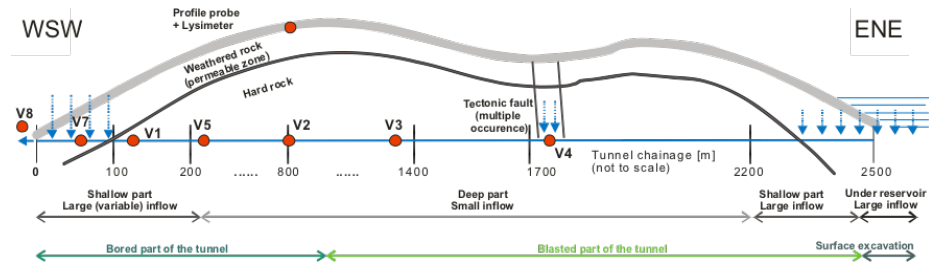


Fig. 1 Schematic cross-section and profile of the Bedrichov Tunnel along with technical and hydrological conditions.

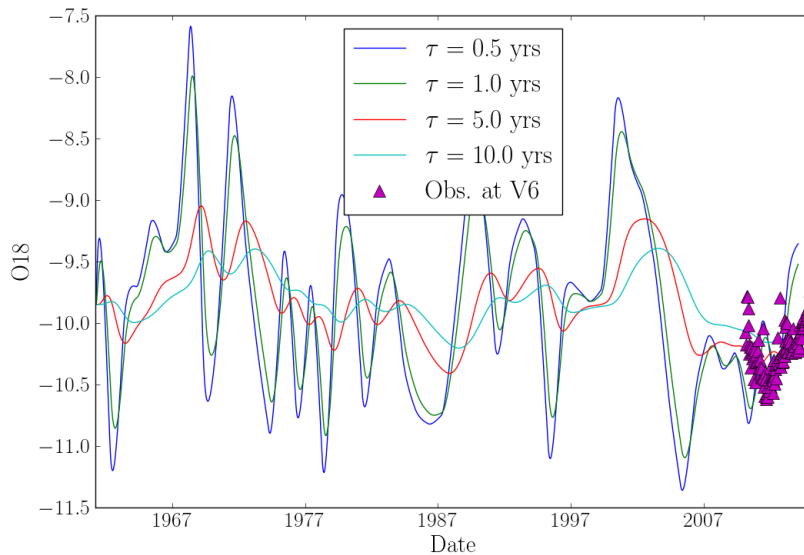


Fig. 2 Effect of increasing mean travel time on the modeled $\delta^{18}\text{O}$ signal using the annual average weighting function and the dispersion TTD for the V6 sampling site along with the observed $\delta^{18}\text{O}$ signal.

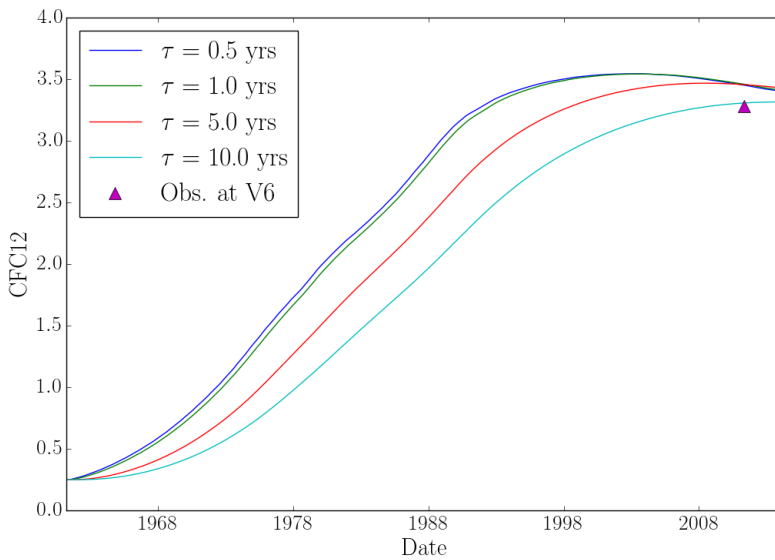


Fig. 3 Effect of increasing mean travel time on the modeled CFC-12 signal using the annual average weighting function and the dispersion TTD for the V6 sampling site along with the observed CFC concentration.

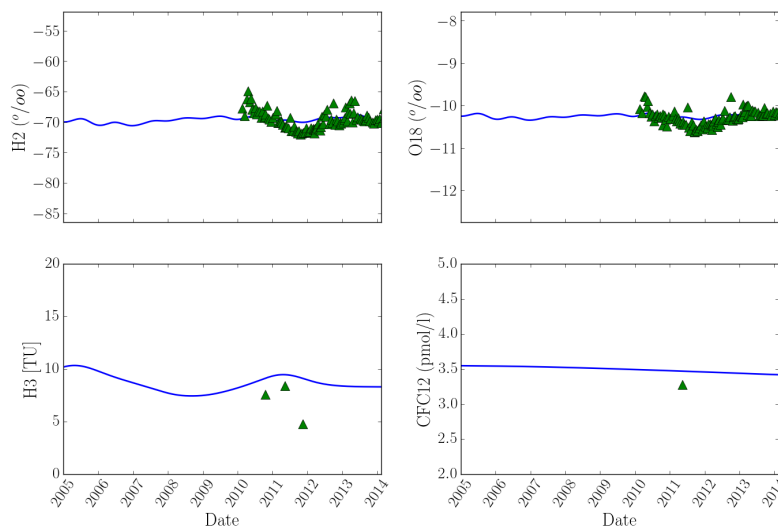


Fig. 4 Tracer data at the V6 sampling location, and the overall multi-tracer best fit lumped parameter model results. For V6 the best fit was achieved for a dispersion TTD using the seasonal input function derived in equation 15.

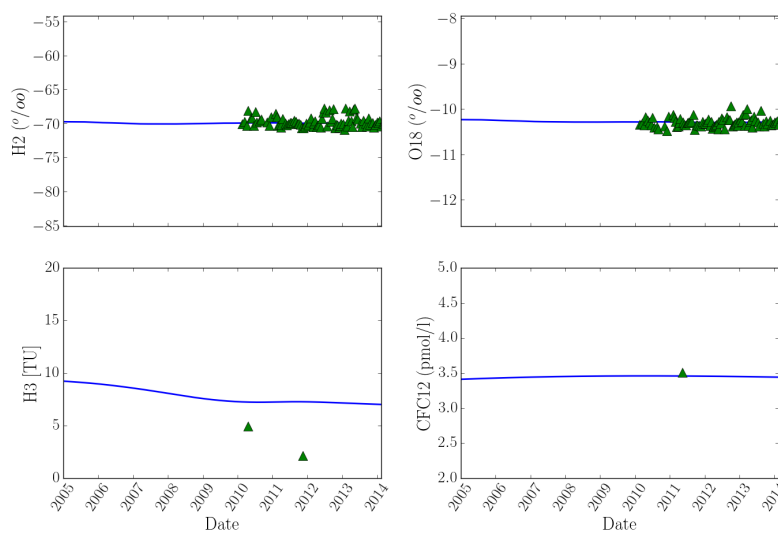


Fig. 5 Tracer data at the V2 sampling location, and the overall multi-tracer best fit lumped parameter model results. For V2 the best fit was achieved for a dispersion TTD using the seasonal input function derived in equation 15.

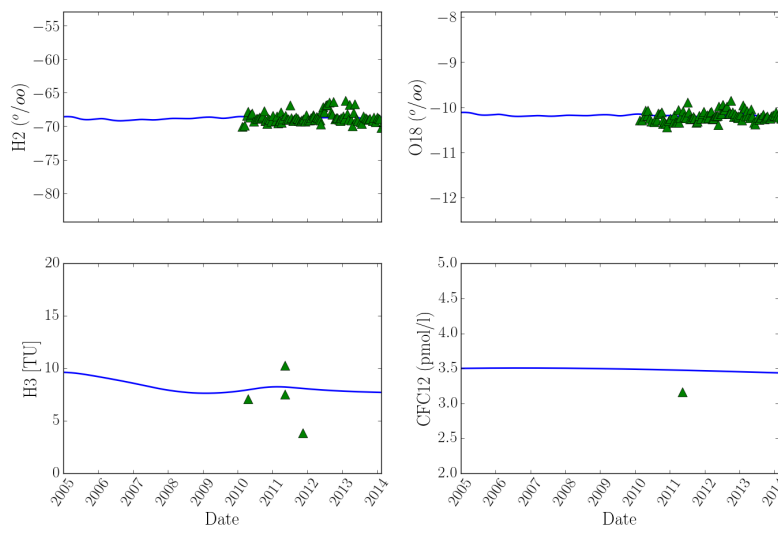


Fig. 6 Tracer data at the V4 sampling location, and the overall multi-tracer best fit lumped parameter model results. For V4 the best fit was achieved for a dispersion TTD using the seasonal input function derived in equation 15.

Table 1 Summary results for V6 sampling site.

| Age Distribution ($g(t)$) | Infil. Func. ($C_{in}(t)$) | τ_{adv} (yr) | +/- (yr) | χ^2 | τ_{tran} yr |
|-----------------------------|------------------------------|-------------------|----------|----------|------------------|
| Dispersive-Matrix Diffusion | Uniform | 2.31 | 0.09 | 573 | 4.73 |
| | eq. 11 | 3.09 | 0.31 | 299 | 6.67 |
| | eq. 14 | 2.62 | 0.15 | 240 | 5.49 |
| | eq. 15 | 2.19 | 0.65 | 200 | 4.45 |
| Dispersive | Uniform | 2.65 | 0.1 | 343 | — |
| | eq. 11 | 7.17 | 0.73 | 283 | — |
| | eq. 14 | 2.58 | 0.15 | 189 | — |
| | eq. 15 | 1.27 | 0.14 | 177 | — |
| Exponential | Uniform | 3.1 | 0.18 | 651 | — |
| | eq. 11 | 5.64 | 0.44 | 328 | — |
| | eq. 14 | 5.78 | 0.55 | 382 | — |
| | eq. 15 | 5.5 | 0.46 | 317 | — |

Table 2 Summary results for V2 sampling site.

| Age Distribution ($g(t)$) | Infil. Func. ($C_{in}(t)$) | τ_{adv} (yr) | +/- (yr) | χ^2 | τ_{tran} yr |
|-----------------------------|------------------------------|-------------------|----------|----------|------------------|
| Dispersive-Matrix Diffusion | Uniform | 2.57 | 0.13 | 575 | 5.37 |
| | eq. 11 | 4.56 | 0.32 | 214 | 10.6 |
| | eq. 14 | 2.83 | 0.2 | 272 | 6.03 |
| | eq. 15 | 3.22 | 1.95 | 107 | 6.99 |
| Dispersive | Uniform | 3.13 | 0.14 | 445 | — |
| | eq. 11 | 8.22 | 0.93 | 202 | — |
| | eq. 14 | 7.32 | 1.07 | 250 | — |
| | eq. 15 | 6.65 | 5.4 | 108 | — |
| Exponential | Uniform | 3.07 | 0.18 | 466 | — |
| | eq. 11 | 7.72 | 0.7 | 226 | — |
| | eq. 14 | 6.66 | 0.77 | 303 | — |
| | eq. 15 | 6.81 | 6 | 111 | — |

Table 3 Summary results for V4 sampling site.

| Age Distribution ($g(t)$) | Infil. Func. ($C_{in}(t)$) | τ_{adv} (yr) | +/- (yr) | χ^2 | τ_{tran} yr |
|-----------------------------|------------------------------|-------------------|----------|----------|------------------|
| Dispersive-Matrix Diffusion | Uniform | 2.22 | 0.09 | 407 | 4.53 |
| | eq. 11 | 4.49 | 0.16 | 210 | 10.4 |
| | eq. 14 | 2.55 | 0.15 | 265 | 5.34 |
| | eq. 15 | 4.62 | 0.22 | 101 | 10.7 |
| Dispersive | Uniform | 3.27 | 0.18 | 372 | — |
| | eq. 11 | 7.08 | 0.76 | 182 | — |
| | eq. 14 | 7.13 | 0.97 | 242 | — |
| | eq. 15 | 3.55 | 1.3 | 96.3 | — |
| Exponential | Uniform | 3.15 | 0.18 | 292 | — |
| | eq. 11 | 7.24 | 0.62 | 224 | — |
| | eq. 14 | 5.62 | 0.54 | 271 | — |
| | eq. 15 | 10.8 | 1.94 | 99.7 | — |

Table 4 Average mean age and standard deviation of mean age estimate for all seasonal input functions given a TTD at each sample location.

| Model | Input func. | τ_{adv} (yr) | σ (yr) | $\bar{\chi}^2$ | σ_χ |
|-------|-----------------------------|-------------------|---------------|----------------|---------------|
| V6 | Dispersive-Matrix Diffusion | 5.33 | 0.993 | 328 | 168 |
| | Dispersive | 3.42 | 2.58 | 248 | 79.1 |
| | Exponential | 5 | 1.28 | 420 | 157 |
| V2 | Dispersive-Matrix Diffusion | 7.24 | 2.31 | 292 | 201 |
| | Dispersive | 6.31 | 2.22 | 251 | 142 |
| | Exponential | 6.06 | 2.05 | 276 | 149 |
| V4 | Dispersive-Matrix Diffusion | 7.74 | 3.26 | 246 | 127 |
| | Dispersive | 5.26 | 2.14 | 223 | 116 |
| | Exponential | 6.7 | 3.21 | 222 | 86.1 |

Table 5 Average mean age and standard deviation of mean age estimate for all TTDs given the seasonal input function at each sample location.

| Model | Input func. | τ_{adv} (yr) | σ (yr) | $\bar{\chi}^2$ | σ_χ |
|-------|-------------|-------------------|---------------|----------------|---------------|
| V6 | Uniform | 3.49 | 1.09 | 522 | 160 |
| | eq. 11 | 6.49 | 0.78 | 303 | 22.8 |
| | eq. 14 | 4.62 | 1.77 | 270 | 100 |
| | eq. 15 | 3.74 | 2.2 | 231 | 75.1 |
| V2 | Uniform | 3.86 | 1.31 | 495 | 69.8 |
| | eq. 11 | 8.83 | 1.52 | 214 | 12 |
| | eq. 14 | 6.67 | 0.645 | 275 | 26.6 |
| | eq. 15 | 6.82 | 0.17 | 109 | 2.08 |
| V4 | Uniform | 3.65 | 0.764 | 357 | 58.9 |
| | eq. 11 | 8.23 | 1.85 | 205 | 21.4 |
| | eq. 14 | 6.03 | 0.963 | 259 | 15.3 |
| | eq. 15 | 8.36 | 4.17 | 99 | 2.43 |

1
2 **References**

3 Bullister JL (2011) Atmospheric CFC-11, CFC-12, CFC-113, CCl4 and SF6 His-
4 tories. Tech. rep., Carbon Dioxide Information Analysis Center, Oak Ridge
5 National Laboratory, US Department of Energy, Oak Ridge, Tennessee, URL
6 http://cdiac.ornl.gov/ftp/oceans/CFC_ATM_Hist/

7 Cook P, Herczeg AL (eds) (2000) Environmental Tracers in Subsurface Hydrology.
8 Kluwer Academic, Norwell, Massachusetts

9 Cook P, Robinson N (2002) Estimating groundwater recharge in fractured rock
10 from environmental H-3 and Cl-36, Clare Valley, South Australia. Water Re-
11 sources Research 38(8), DOI 10.1029/2001WR000772

12 Cook P, Love A, Robinson N, Simmons C (2005) Ground-
13 water ages in fractured rock aquifers. Journal of Hydrol-
14 ogy 308(1-4):284 – 301, DOI 10.1016/j.jhydrol.2004.11.005, URL
15 <http://www.sciencedirect.com/science/article/pii/S0022169404005360>

16 Danckwerts P (1953) Continuous flow systems. Chemical Engineering Sci-
17 ence 2(1):1 – 13, DOI [http://dx.doi.org/10.1016/0009-2509\(53\)80001-1](http://dx.doi.org/10.1016/0009-2509(53)80001-1), URL
18 <http://www.sciencedirect.com/science/article/pii/0009250953800011>

19 Doyon B, Molson JW (2012) Groundwater age in fractured porous me-
20 dia: Analytical solution for parallel fractures. Advances in Water Resources
21 37:127 – 135, DOI <http://dx.doi.org/10.1016/j.advwatres.2011.11.008>, URL
22 <http://www.sciencedirect.com/science/article/pii/S030917081100220X>

23 Evaristo J, Jasechko S, McDonnell JJ (2015) Global separation of plant tran-
24 spiration from groundwater and streamflow. Nature 525(7567):91–94, URL
25 <http://dx.doi.org/10.1038/nature14983>

26 Gardner WP, Susong DD, Solomon DK, Heasler HP (2010) Snowmelt
27 hydrograph interpretation: Revealing watershed scale hydrologic char-
28 acteristics of the Yellowstone Volcanic Plateau. Journal of Hy-
29 drology 383(3-4):209–222, DOI DOI: 10.1016/j.jhydrol.2009.12.037,
30 URL <http://www.sciencedirect.com/science/article/B6V6C-4Y34R3F-4/2/7600ad03d1d63fef58766bc7aa7d0b3>

31 Gardner WP, Susong DD, Solomon DK, Heasler HP (2011) A multitracer
32 approach for characterizing interactions between shallow groundwater and
33 the hydrothermal system in the Norris Geyser Basin area, Yellowstone
34 National Park. Geochemistry Geophysics Geosystems 12(8):Q08,005, URL
35 <http://dx.doi.org/10.1029/2010GC003353>

36 Haggerty R, Gorelick SM (1995) Multiple-rate mass transfer for modeling diffusion
37 and surface reactions in media with pore-scale heterogeneity. Water Resources
38 Research 31(10):2383–2400, URL <http://dx.doi.org/10.1029/95WR10583>

39 Haggerty R, McKenna SA, Meigs LC (2000) On the late-time behavior of tracer
40 test breakthrough curves. Water Resources Research 36(12):3467–3479, URL
41 <http://dx.doi.org/10.1029/2000WR900214>

42 Haggerty R, Fleming SW, Meigs LC, McKenna SA (2001) Tracer tests
43 in a fractured dolomite: 2. analysis of mass transfer in single-well
44 injection-withdrawal tests. Water Resources Research 37(5):1129–1142, URL
45 <http://dx.doi.org/10.1029/2000WR900334>

46 Kennedy V, Kendall C, Zellweger G, Wyerman T, Avanzino R (1986) De-
47 termination of the components of stormflow using water chemistry and en-
48 vironmental isotopes, mattole river basin, california. Journal of Hydrology
49

50

51

52

53

54

55

56

57

58

59

60

61

62

63

64

65

1 84(12):107 – 140, DOI [http://dx.doi.org/10.1016/0022-1694\(86\)90047-8](http://dx.doi.org/10.1016/0022-1694(86)90047-8), URL
2 <http://www.sciencedirect.com/science/article/pii/0022169486900478>

3 Maloszewski P, Zuber A (1982) Determining the turnover time of groundwa-
4 ter systems with the aid of environmental tracers. *Journal of Hydrology*
5 57(3):207 – 231, DOI [http://dx.doi.org/10.1016/0022-1694\(82\)90147-0](http://dx.doi.org/10.1016/0022-1694(82)90147-0), URL
6 <http://www.sciencedirect.com/science/article/pii/0022169482901470>

7 Maloszewski P, Zuber A (1985) On the theory of tracer experiments in
8 fissured rocks with a porous matrix. *Journal of Hydrology* 79(3):333
9 – 358, DOI [http://dx.doi.org/10.1016/0022-1694\(85\)90064-2](http://dx.doi.org/10.1016/0022-1694(85)90064-2), URL
10 <http://www.sciencedirect.com/science/article/pii/0022169485900642>

11 Maloszewski P, Zuber A (1990) Mathematical modeling of tracer be-
12 havior in short-term experiments in fissured rocks. *Water Resources*
13 Research 26(7):1517–1528, DOI 10.1029/WR026i007p01517, URL
14 <http://dx.doi.org/10.1029/WR026i007p01517>

15 Maloszewski P, Zuber A (1996) Lumped parameter models for the interpretation
16 of environmental tracer data. IAEA Technical Report

17 McCallum JL, Engdahl NB, Ginn TR, Cook PG (2014) Nonparametric
18 estimation of groundwater residence time distributions: What can envi-
19 ronmental tracer data tell us about groundwater residence time? *Wa-
20 ter Resources Research* pp n/a–n/a, DOI 10.1002/2013WR014974, URL
21 <http://dx.doi.org/10.1002/2013WR014974>

22 Neretnieks I (1980) Diffusion in the rock matrix: An important fac-
23 tor in radionuclide retardation? *Journal of Geophysical Research: Solid*
24 *Earth* 85(B8):4379–4397, DOI 10.1029/JB085iB08p04379, URL
25 <http://dx.doi.org/10.1029/JB085iB08p04379>

26 Neretnieks I (1981) Age dating of groundwater in fissured rock:
27 Influence of water volume in micropores. *Water Resources Re-
28 search* 17(2):421–422, DOI 10.1029/WR017i002p00421, URL
29 <http://dx.doi.org/10.1029/WR017i002p00421>

30 Neuman S (2005) Trends, prospects and challenges in quantifying flow and
31 transport through fractured rocks. *Hydrogeology Journal* 13(1):124–147, DOI
32 10.1007/s10040-004-0397-2, URL <http://dx.doi.org/10.1007/s10040-004-0397-2>

33 Painter S, Cvetkovic V (2005) Upscaling discrete fracture network simulations:
34 An alternative to continuum transport models. *Water Resources Research*
35 41(2):W02,002–, URL <http://dx.doi.org/10.1029/2004WR003682>

36 Painter S, Cvetkovic V, Mancillas J, Pensado O (2008) Time domain
37 particle tracking methods for simulating transport with retention and
38 first-order transformation. *Water Resources Research* 44(1):W01,406–, URL
39 <http://dx.doi.org/10.1029/2007WR005944>

40 Roubinet D, de Dreuzy JR, Tartakovsky DM (2013) Particle-tracking simulations
41 of anomalous transport in hierarchically fractured rocks. *Computers & Geo-
42 sciences* 50:52 – 58, DOI <http://dx.doi.org/10.1016/j.cageo.2012.07.032>, URL
43 <http://www.sciencedirect.com/science/article/pii/S0098300412002774>, bench-
44 mark problems, datasets and methodologies for the computational geosciences

45 Shapiro AM (2001) Effective matrix diffusion in kilometer-scale transport in
46 fractured crystalline rock. *Water Resources Research* 37(3):507–522, DOI
47 10.1029/2000WR900301, URL <http://dx.doi.org/10.1029/2000WR900301>

48 Solomon DK, Genereux DP, Plummer LN, Busenberg E (2010) Testing mix-
49 ing models of old and young groundwater in a tropical lowland rain for-
50

51

52

53

54

55

56

57

58

59

60

61

62

63

64

65

1 est with environmental tracers. *Water Resour Res* 46(4):W04,518–, URL
2 <http://dx.doi.org/10.1029/2009WR008341>

3 Solomon DK, Gilmore TE, Solder JE, Kimball B, Genereux DP (2015) Evaluating
4 an unconfined aquifer by analysis of age-dating tracers in stream water. *Wa-
5 ter Resources Research* 51(11):8883–8899, DOI 10.1002/2015WR017602, URL
6 <http://dx.doi.org/10.1002/2015WR017602>

7 Sudicky EA, Frind EO (1982) Contaminant transport in fractured porous
8 media: Analytical solutions for a system of parallel fractures. *Water Re-
9 sources Research* 18(6):1634–1642, DOI 10.1029/WR018i006p01634, URL
10 <http://dx.doi.org/10.1029/WR018i006p01634>

11 Tang DH, Frind EO, Sudicky EA (1981) Contaminant transport in frac-
12 tured porous media: Analytical solution for a single fracture. *Water Re-
13 sources Research* 17(3):555–564, DOI 10.1029/WR017i003p00555, URL
14 <http://dx.doi.org/10.1029/WR017i003p00555>

15 Therrien R, Sudicky E (1996) Three-dimensional analysis of variably-saturated
16 flow and solute transport in discretely-fractured porous media. *Journal of Con-
17 taminant Hydrology* 23(1-2):1 – 44, DOI 10.1016/0169-7722(95)00088-7, URL
18 <http://www.sciencedirect.com/science/article/pii/0169772295000887>

19 Thoma MJ, McNamara JP, Gribb MM, Benner SG (2011) Seasonal
20 recharge components in an urban/agricultural mountain front aquifer
21 system using noble gas thermometry. *Journal of Hydrology* 409(12):118
22 – 127, DOI <http://dx.doi.org/10.1016/j.jhydrol.2011.08.003>, URL
23 <http://www.sciencedirect.com/science/article/pii/S0022169411005294>

24 Warren J, Root P (1963) The behavior of naturally fractured reservoirs. *Society
25 of Petroleum Engineers* pp –

26 Weiss R (1968) Piggyback sampler for dissolved gas studies on sealed water sam-
27 ples. *Deep Sea Research and Oceanographic Abstracts* 15(6):695 – 699

28 Zak J, Verner K, Klominsky J, Chlupacova M (2009) “Granite tectonics” revisited:
29 insights from comparison of K-feldspar shape-fabric, anisotropy of magnetic sus-
30 ceptibility (AMS), and brittle fractures in the Jizera granite, Bohemian Massif.
31 *International Journal of Earth Sciences* 98(5):949–967

32 Zuber A, Maloszewski P (2001) Environmental Isotopes in the Hydrologic Cycle,
33 IHP-V Technical Documents in Hydrology, vol 6. International Atomic Energy
34 Agency

35

36

37

38

39

40

41

42

43

44

45

46

47

48

49

50

51

52

53

54

55

56

57

58

59

60

61

62

63

64

65